CVEL

THE CLEMSON UNIVERSITY VEHICULAR ELECTRONICS LABORATORY

TECHNICAL REPORT: CVEL-17-068

Evaluation of the Common Mode Voltage Generated by Different CAN Transceivers

Jongtae Ahn and Dr. Todd Hubing

Clemson University

March 20, 2018

Table of Contents

Abstract

Controller Area Network (CAN) signaling is differential; however unintended common-mode components of the signal can contribute to unintentional conducted and radiated emissions. In this report, five CAN transceivers are evaluated to determine how much common-mode voltage they produce in various circumstances.

1. Introduction

The common-mode (CM) component of differential signals often plays a key role in unintended conducted and radiated emissions. The pseudo-differential drivers generally used to produce balanced digital signals create a CM voltage component whenever the timing of the high-to-low and low-to-high transitions is not exactly the same.

Controller Area Network (CAN) is a network protocol widely used in the automotive industry. CAN employs analog circuit techniques to provide data transfers up to 1 Mb/s, and is a relatively low cost, low power networking option that has good noise immunity [1]. Researchers have investigated the electromagnetic immunity of CAN transceivers, and developed circuit-modeling procedures for signal immunity simulation [2]-[5]; but the electromagnetic emissions from modern CAN sources has not been investigated. Many automotive electronics suppliers offer CAN transceivers that meet the specifications of the CAN standard [6]. However CAN transceivers from different OEMs can exhibit significant differences in important characteristics not specified by the standard such as maximum slew rate and CM voltage.

Differential voltages and currents produce fields that are largely self-canceling, and perfectly differential signals are not good sources of conducted and radiated emissions [2]. On the other hand, imbalances in the differential signaling can introduce CM components resulting in EMI problems [7]-[12]. An analysis of source imbalances in differential signaling was conducted by Chen et al [11]. Hans-Werner et al showed that the EMC of in-vehicle multiplex networks is largely determined by the EMC

of the transceiver ICs [13]. This paper describes measurements comparing different CAN transceivers to evaluate sources of imbalance that produce common-mode components in their signal outputs.

2. Test setup for measuring CM voltages produced by a CAN driver

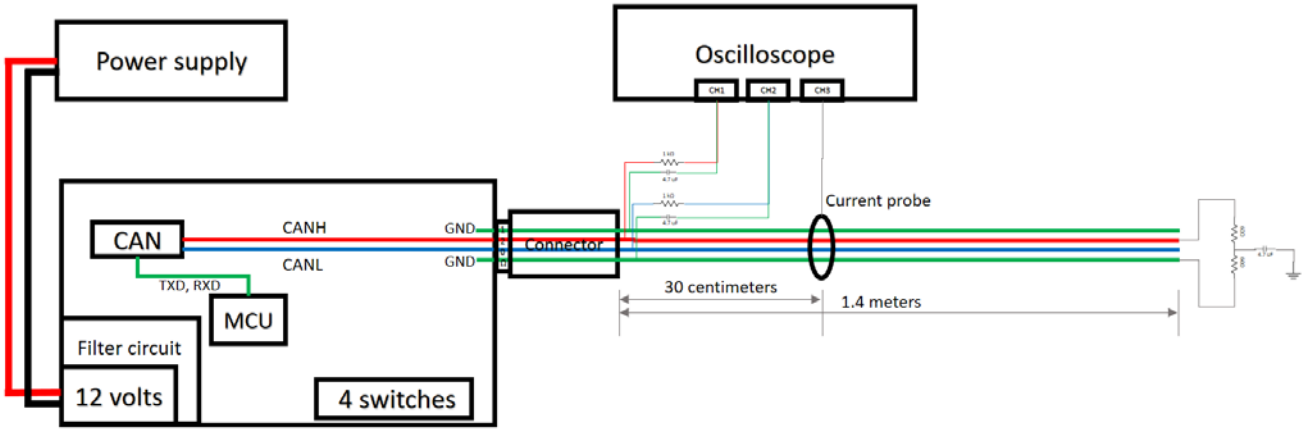

Fig. 1. Schematic view of CAN transceiver test set-up.

A test fixture was designed to evaluate the signals produced by various CAN transceivers. The test setup is schematically illustrated in Fig. 1. The CAN transceiver is mounted to a 20×15 cm printed circuit board (PCB). Five identical circuit boards were built; one for each transceiver evaluated. The PCBs were powered by an external 12-volt DC supply. An NXP S912ZVC19F0MKHR microcontroller drives the transceiver. Four switches on each board are used to adjust the baud rate of the CAN transceiver. The differential signal traces, CANH and CANL, are routed across the board to a D-sub connector. The 5-volt power to the transceiver is supplied by the microcontroller. A 1.4-meter wire harness consisting of a twisted wire pair and two ground wires is attached to the D-sub connector. A 120-ohm differential termination is located on the wire harness at the connector. Another 120-ohm split termination (two 60-ohm resistors to ground) is located at the far end of the twisted wire pair.

A Fischer Custom Communications current probe (F-33-1) was used to measure CM current on the twisted wire pair. The CM current was measured 30 centimeters away from the connector. 21:1 probes for measuring the differential signals were built into the connector assembly. The probes consisted of 1-kohm resistors in series with the 50-ohm coaxial cables attached to the oscilloscope. The shields of the

coaxial cables were connected to circuit ground through 4.7 μF capacitors to prevent low-frequency signal currents from returning through the oscilloscope ground. The probes were integrated with the connector assembly so that each transceiver board could be measured using the same probes.

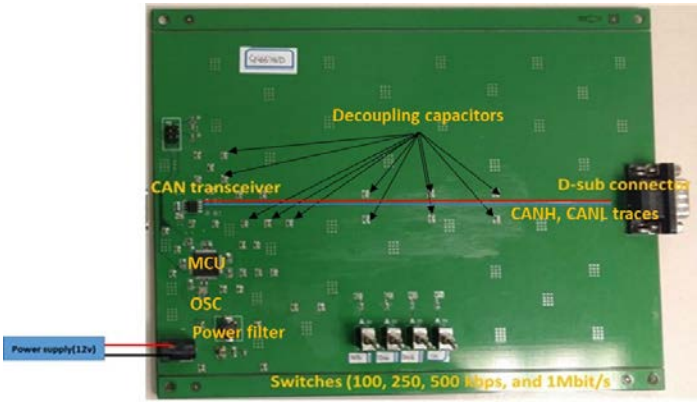

Fig. 2. The fabricated printed circuit board top view

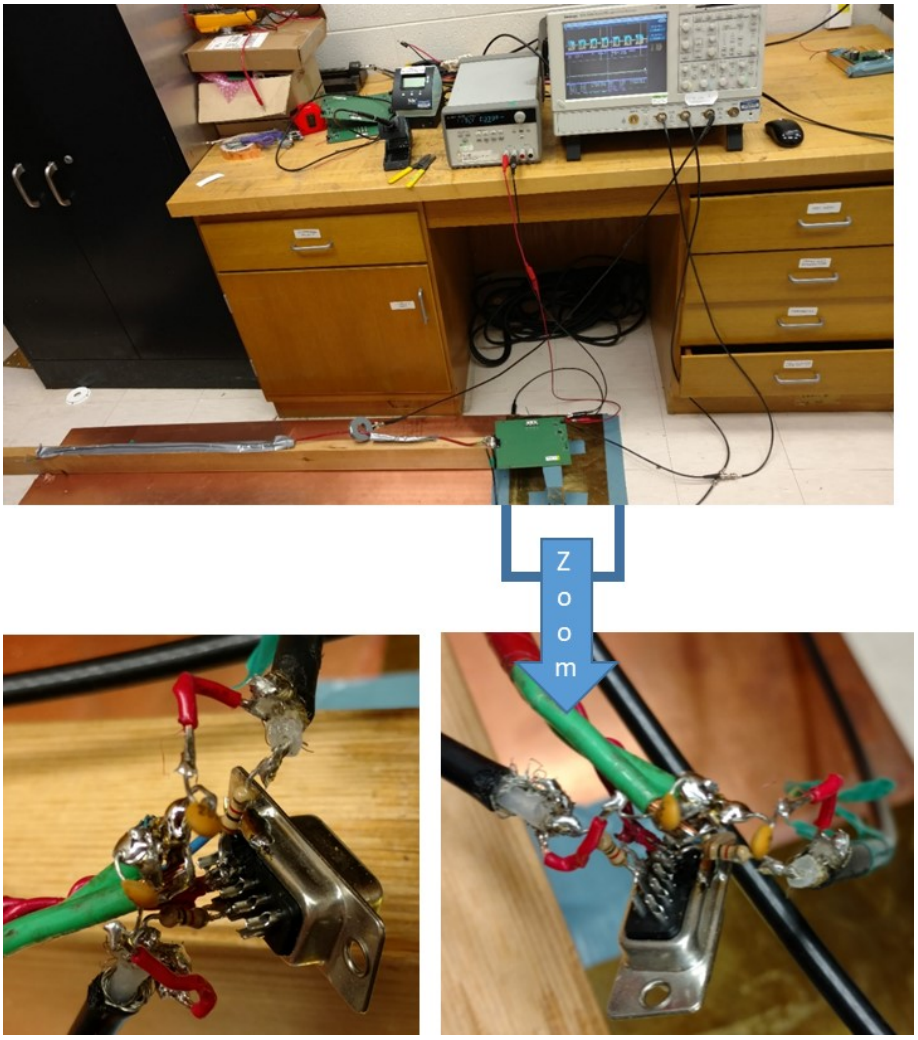

Fig. 3. Test set-up and probe connection configuration

The PCB and the test set-up are shown in Fig. 2 and Fig. 3, respectively. Forty decoupling capacitors are mounted on the PCB to minimize power-bus noise. Four switches on the PCB are used to set the baud rate to 100 kb/s, 250 kb/s, 500 kb/s, or 1 Mb/s. Five PCBs were fabricated with exactly the same design. Five CAN transceivers were selected with identical packaging: “A” and “B” from the same company, “C”, “D”, and “E” from three other companies. The wire harness consisted of a twisted wire pair (AWG18) and two ground wires (AWG12). The length of the wire harness was 1.4 m and the differential signal traces on the PCB were 17 cm long. The voltage on each of the wires in the twisted pair (relative to ground) was measured at the connector.

3. Experiment results

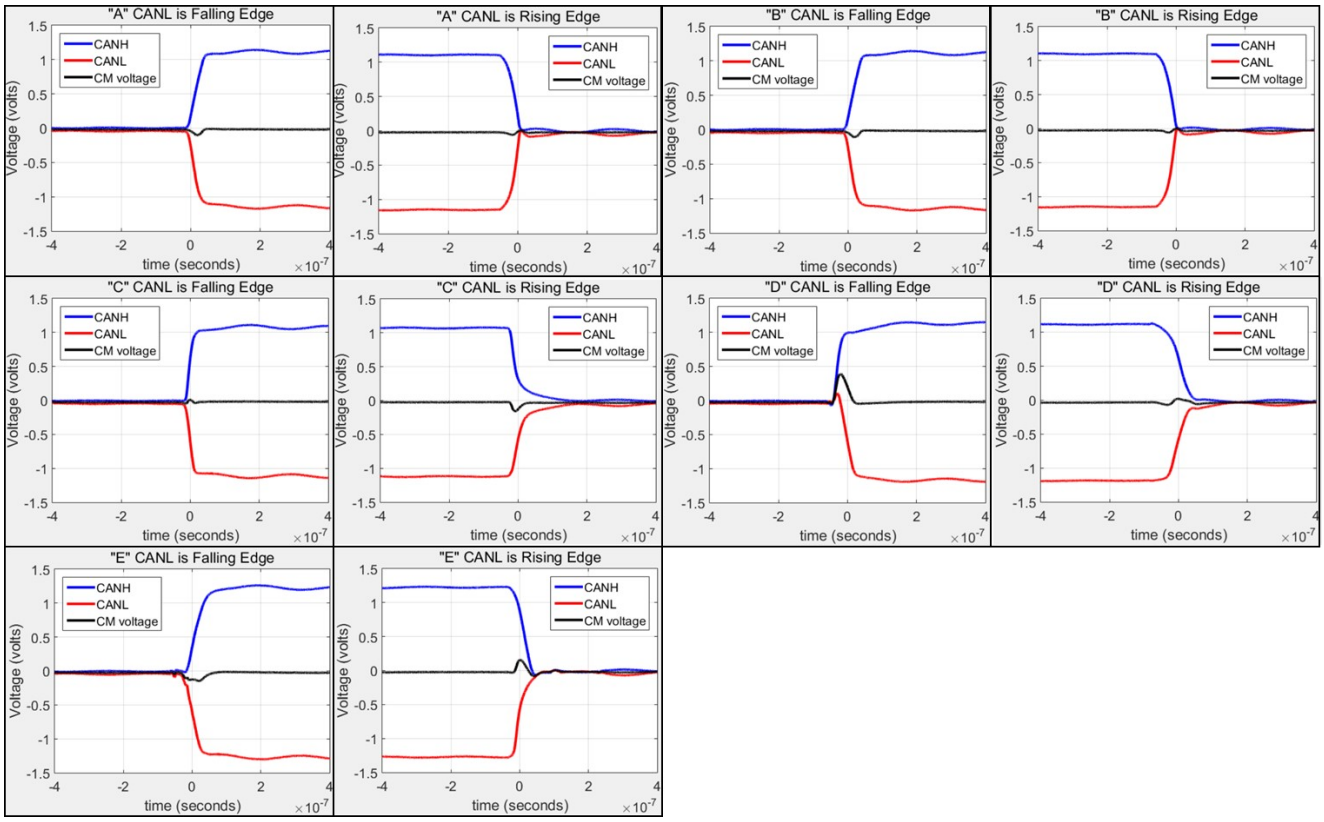

Fig. 4. Measured differential signal voltage and common-mode voltage for the five transceivers

Nominally, the CM voltage in a CAN signal is a constant DC value of approximately 2.5 volts. In these measurements, the 4.7-μF capacitor filters out the DC component of the CM voltage. Nonzero fluctuations in the CM component of the signal arise due to signal asymmetries such as amplitude

mismatches between V_1 and V_2 rise- and fall-time mismatches, or time offsets between the transitions of the two single-ended signals (skew) [10].

The voltages measured on the CANH and CANL wires for each of the transceivers are shown in Fig. 4. The sum of these voltages, the common-mode voltage, is also shown. The baud rate in this case is 1 Mb/s, which is highest speed for the given transceivers. The CM voltage is highest during the transition of the differential voltage. The measured differential signal voltages are approximately 0 or 2.2 volts, depending on the state of the output. In this test, the “A” and “B” transceivers generate smaller CM voltages than the other transceivers because their signals are more symmetric. Generally, the amplitude of the CM voltage was different on low-to-high transitions than it was on high-to-low transitions. This was particularly the case with the “D” transceiver.

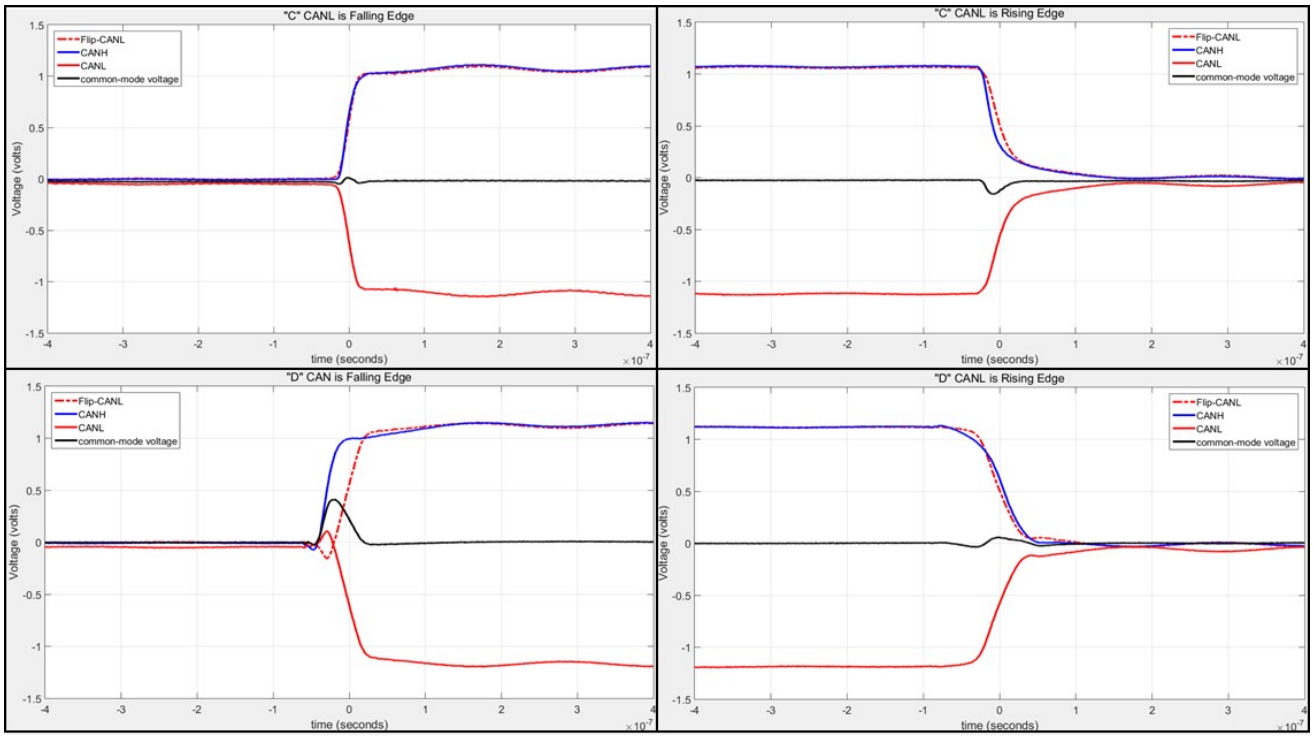

Fig. 5. Slew rates and time offset in the transition

Fig. 5 shows the differential signals for the “C” and “D” transceivers with the CANL signal inverted to illustrate differences in the timing and slew-rate that result in the CM voltage. The dominant source of CM voltage in the “A”, “B” and “C” transceivers was the difference in the slew rates. The “D”

transceiver, however, has a time offset between transitions when CANL is falling. That is resulted in the worst CM voltage generated by any of the five transceivers evaluated.

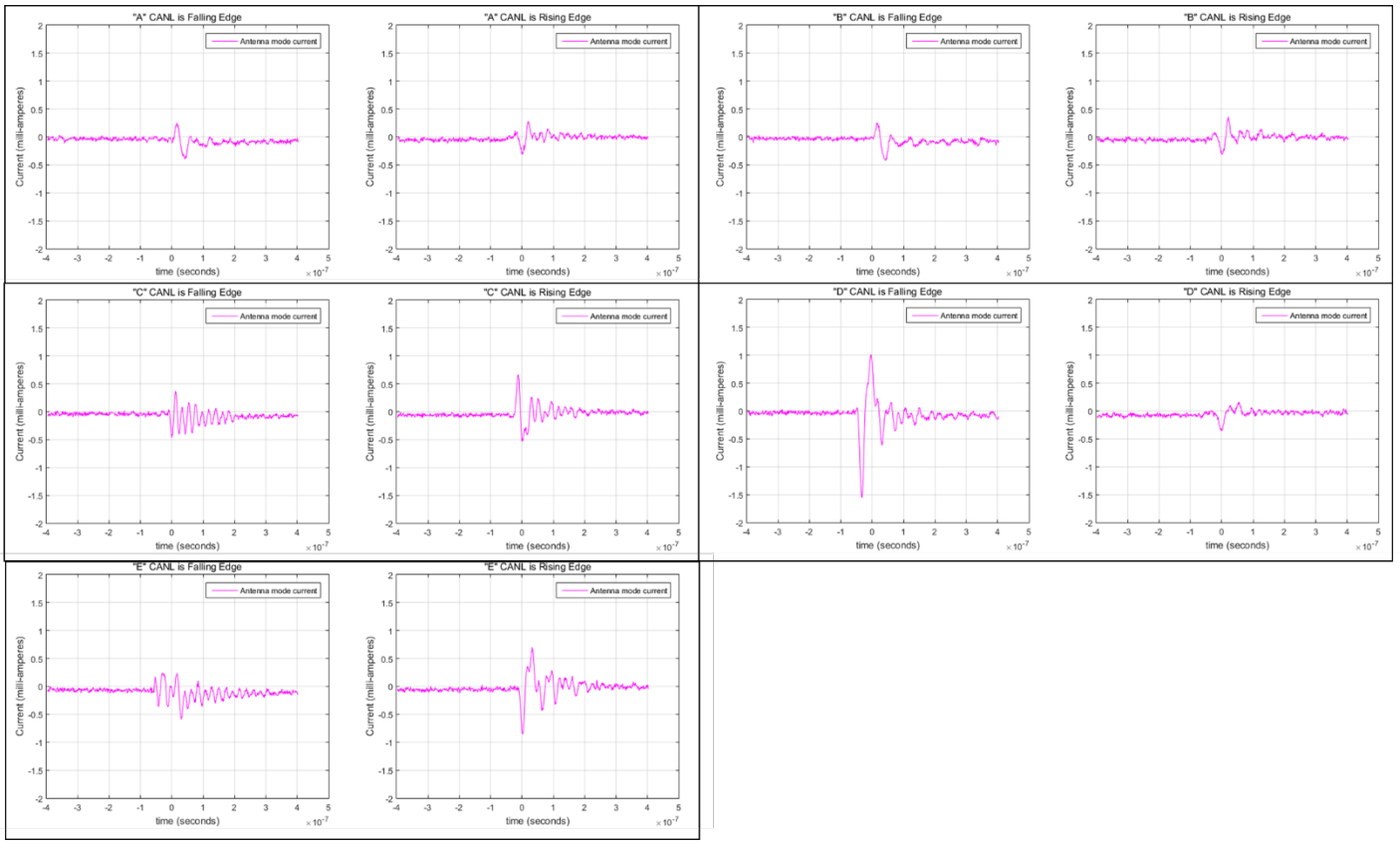

Fig. 6. Common-mode currents measurements for the five transceivers

The CM voltage on the twisted wire pair produces a CM current. The CM current measured with the F-33-1 probe for each transceiver on both rising and falling transitions is shown in Fig. 6. The baud rate is 1 Mb/s.

The peak CM current for each transceiver was recorded. For example, as indicated in the plots, the peak value of the measured CM current is -0.48 mA for transceiver “A” on the rising edge and 0.44 mA for transceiver “B” on the falling edge. The fall time of the “C” transceiver is much faster than the other transceivers, so even though the peak CM voltage is not high, the energy in the CM voltage waveform is high enough to generate significant CM current.

Generally, the results show that higher CM voltages generated higher CM currents. The ringing in the CM current waveforms is due to the CM impedance of the wire harness structure, which is largely determined by the length of the harness and its CM terminations.

Table 1. Measured transition times and CM voltage peaks and CM current peaks

CANL is falling edge		Rising/Falling time	CM voltage (pk)	CM Currents (pk)
"A"	100kHz	37 ns / 39 ns	-88 mV	0.44 mA
	250kHz	37 ns / 39 ns	-89 mV	0.42 mA
	500kHz	38 ns / 34 ns	-84 mV	0.43 mA
	1 MHz	38 ns / 34 ns	-83 mV	0.43 mA
"B"	100kHz	37 ns / 33 ns	-95 mV	0.44 mA
	250kHz	38 ns / 34 ns	-95 mV	0.44 mA
	500kHz	38 ns / 40 ns	-92 mV	0.46 mA
	1 MHz	39 ns / 34 ns	-87 mV	0.48 mA
"C"	100kHz	27 ns / 20 ns	61 mV	-0.77 mA
	250kHz	26 ns / 23 ns	50 mV	-0.70 mA
	500kHz	26 ns / 21 ns	46 mV	0.68 mA
	1 MHz	22 ns / 24 ns	38 mV	0.69 mA
"D"	100kHz	85 ns / 39 ns	424 mV	1.5 mA
	250kHz	84 ns / 38 ns	419 mV	1.5 mA
	500kHz	86 ns / 39 ns	416 mV	1.6 mA
	1 MHz	81 ns / 38 ns	413 mV	1.5 mA
"E"	100kHz	52 ns / 49 ns	-124 mV	-0.39 mA
	250kHz	53 ns / 47 ns	-122 mV	-0.38 mA
	500kHz	52 ns / 45 ns	-124 mV	-0.38 mA
	1 MHz	52 ns / 50 ns	-125 mV	-0.44 mA

CANL is rising edge		Rising/Falling time	CM voltage (pk)	CM Currents (pk)
"A"	100kHz	35 ns / 37 ns	-39 mV	-0.48 mA
	250kHz	34 ns / 37 ns	40 mV	-0.47 mA
	500kHz	34 ns / 37 ns	-41 mV	-0.47 mA
	1 MHz	35 ns / 38 ns	-39 mV	-0.48 mA
"B"	100kHz	36 ns / 38 ns	-35 mV	-0.43 mA
	250kHz	35 ns / 37 ns	-35 mV	-0.46 mA
	500kHz	35 ns / 38 ns	38 mV	-0.46 mA
	1 MHz	35 ns / 38 ns	37 mV	-0.47 mA
"C"	100kHz	70 ns / 64 ns	-134 mV	0.66 mA
	250kHz	69 ns / 70 ns	-135 mV	0.66 mA
	500kHz	71 ns / 60 ns	-134 mV	0.66 mA
	1 MHz	62 ns / 66 ns	-135 mV	0.66 mA
"D"	100kHz	52 ns / 67 ns	52 mV	-0.34 mA
	250kHz	52 ns / 70 ns	55 mV	-0.32 mA
	500kHz	53 ns / 67 ns	53 mV	-0.35 mA
	1 MHz	57 ns / 67 ns	59 mV	-0.34 mA
"E"	100kHz	50 ns / 44 ns	-185 mV	-0.95 mA
	250kHz	50 ns / 44 ns	-184 mV	-0.93 mA
	500kHz	51 ns / 44 ns	-182 mV	-0.96 mA
	1 MHz	51 ns / 43 ns	-183 mV	-0.95 mA

Similar measurements were made on each transceiver at each of the four baud rates and the results are summarized in Table 1. Each CAN transceiver tested produced a differential signal complying with the CAN standard [14]. Each transceiver tested appeared to control the rise and fall times of the signal, which ranged from 20 nsec to 86 nsec. Nevertheless, on some transceivers the rise-times were significantly different from the fall-times. Peak CM voltage magnitudes ranged from 35 mV to 419 mV, and peak CM current magnitudes ranged from 0.32 mA to 1.6 mA.

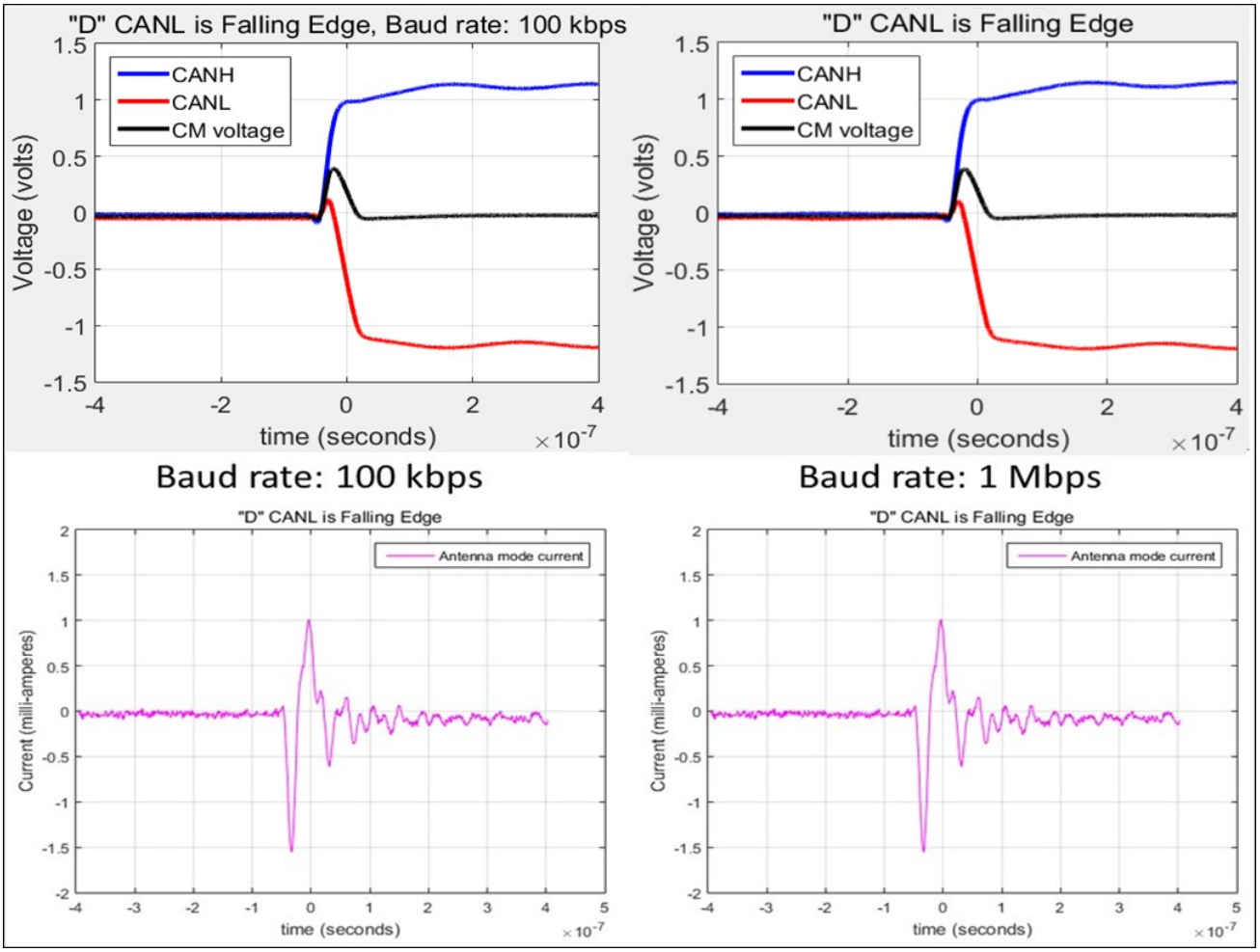

Fig. 7. Common mode voltages and currents at different baud rates

No significant difference in the CM voltages or currents was observed when varying the baud rate of a given transceiver. For example, Fig. 7shows the waveforms measured on transceiver “D” at 100 kbps and 1 Mbps.

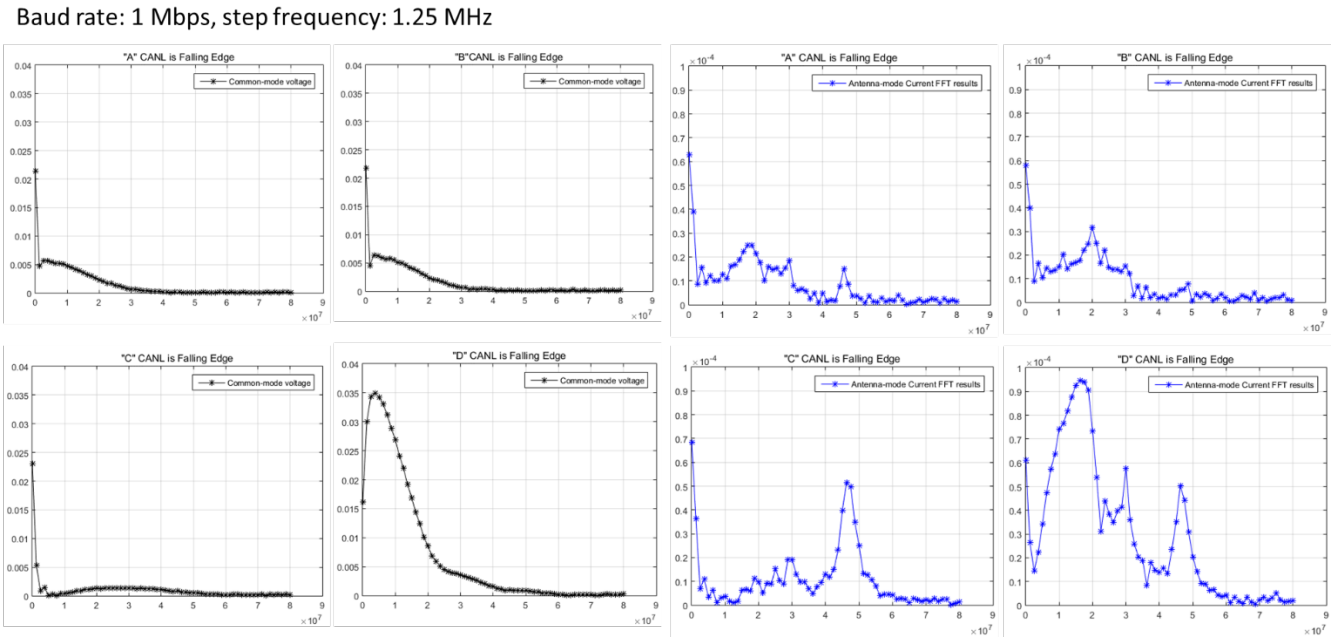

Fig. 8. Frequency domain representation of the common-mode voltages and currents

The Fourier transform (FFT) of the CM voltage and current waveforms was calculated for four of the measured waveforms and is shown in Fig. 8. The CM currents exhibit peaks at frequencies corresponding to resonances of the wire harness. When the CM voltage is strong enough to excite the wire harness, the corresponding CM currents peaks appear at the resonant frequencies. The “A” and “B” transceivers generate CM voltages that have more energy at 20 MHz than they do at 40 MHz and higher. These pulses excite a system resonance at around 20 MHz. The “C” and “D” transceivers generate CM pulses with significant energy above 40 MHz and excite a system resonance at around 46 MHz. On the CANL falling edge, the “D” transceiver exhibited a timing offset that generated significant low-frequency energy. This drives the resonance just below 20 MHz much more strongly than the other pulses.

4. Conclusion

In this paper, the CM voltages generated by five different CAN transceivers were evaluated. All of the transceivers met the functional requirements of the CAN specification. Each of the transceivers appeared to control the rise and fall times, which ranged from 20 nsec to 86 nsec. Some transceivers did a poor job of matching the rise and fall times resulting in significant common-mode voltage fluctuations during transitions. The CM voltage fluctuations did not appear to be dependent on the baud rate. The

analysis of the common-mode currents indicates that the resonant frequencies were mainly determined by the CM impedance of the harness, not by the common-mode fluctuations, which tended to be relatively wide-band pulses. Nevertheless, the frequency content of the CM voltages did influence which system resonances were excited most strongly.

References

[1] H. Bauer, *Automotive Electrics/Automotive Electronics*. vol. 4, John Wiley & Sons, 2004.

[2] M. Fontana, F. G. Canavero and R. Perraud, "Integrated circuit modeling for noise susceptibility prediction in communication networks," *IEEE Trans. Electromagn. Compat.*, vol. 57, no.3, pp. 339-348, 2015.

[3] J. Koo et al, "A nonlinear microcontroller power distribution network model for the characterization of immunity to electrical fast transients," *IEEE Trans. Electromagn. Compat.*, vol. 51, no.3, pp. 611-619, 2009.

[4] J. Zhang et al, "Modeling of the immunity of ICs to EFTs," in Electromagnetic Compatibility (EMC), 2010 IEEE International Symposium On, 2010.

[5] M. Fontana and T. H. Hubing, "Characterization of CAN network susceptibility to EFT transient noise," *IEEE Trans. Electromagn. Compat.*, vol. 57, no.2, pp. 188-194, 2015.

[6] International Electrotechnical Commission, "CISPR 25 limits and methods of measurement of radio disturbance characteristics for the protection of receivers used on board vehicles," Geneva: International Electrotechnical Commission, 1995.

[7] B. Archambeault et al, "Electromagnetic radiation resulting from PCB/high-density connector interfaces," *IEEE Trans. Electromagn. Compat.*, vol. 55, no.4, pp. 614-623, 2013.

[8] L. Niu and T. H. Hubing, "Rigorous derivation of imbalance difference theory for modeling radiated emission problems," *IEEE Trans. Electromagn. Compat.*, vol. 57, no.5, pp. 1021-1026, 2015.

[9] M. Sørensen, T. H. Hubing and K. Jensen, "Study of the impact of board orientation on radiated emissions due to common-mode currents on attached cables," in Electromagnetic Compatibility (EMC), 2016 IEEE International Symposium On, 2016, .

[10] C. R. Paul, "A comparison of the contributions of common-mode and differential-mode currents in radiated emissions," *IEEE Trans. Electromagn. Compat.*, vol. 31, no.2, pp. 189-193, 1989.

[11] C. Wang and J. L. Drewniak, "Quantifying the effects on EMI and SI of source imbalances in differential signaling," in Electromagnetic Compatibility, 2003 IEEE International Symposium On, 2003.

[12] H. Kwak and T. H. Hubing, "Investigation of the imbalance difference model and its application to various circuit board and cable geometries," in Electromagnetic Compatibility (EMC), 2012 IEEE International Symposium On, 2012.

[13] H. Luetjens and H. Eisele, "How to qualify EMC in multiplexing," SAE International, 1999.

[14] R. Bosch, "CAN specification version 2.0," 1991.